Cell, Vol. 110, 457–466, August 23, 2002, Copyright ©2002 by Cell Press

The *Drosophila Hox* Gene *Deformed* Sculpts Head Morphology via Direct Regulation of the Apoptosis Activator *reaper*

Ingrid Lohmann, Nadine McGinnis, Morana Bodmer, and William McGinnis[1]
Section of Cell and Developmental Biology
University of California, San Diego
La Jolla, California 92093

Summary

Hox proteins control morphological diversity along the anterior-posterior body axis of animals, but the cellular processes they directly regulate are poorly understood. We show that during early *Drosophila* development, the Hox protein Deformed (Dfd) maintains the boundary between the maxillary and mandibular head lobes by activating localized apoptosis. Dfd accomplishes this by directly activating the cell death promoting gene *reaper* (*rpr*). One other *Hox* gene, *Abdominal-B* (*Abd-B*), also regulates segment boundaries through the regional activation of apoptosis. Thus, one mechanism used by *Drosophila Hox* genes to modulate segmental morphology is to regulate programmed cell death, which literally sculpts segments into distinct shapes. This and other emerging evidence suggests that Hox proteins may often regulate the maintenance of segment boundaries.

Introduction

During the development of *Drosophila*, *Hox* genes are expressed in specific domains along the anterior-posterior (A/P) body axis and assign different identities and morphologies to segments in the head, thorax, and abdomen (Figure 1A; Mann and Morata, 2000). At the molecular level, *Hox* genes encode homeodomain transcription factors and diversify segmental features by the regulation of a complex set of downstream genes (Graba et al., 1997). It has been long recognized that Hox proteins will regulate cytodifferentiation processes by controlling a battery of subordinate targets, the *Hox* realizator genes (Garcia-Bellido, 1977), which directly influence mitotic rates, cell-cell adhesion, cell shape, cell migration, and cell death. Although some of these cellular processes and a few potential realizator genes are known to be dependent on the activity of *Hox* genes (Pradel and White, 1998; Hu and Castelli-Gair, 1999), how or whether they are directly controlled by *Hox* genes is not yet known.

Programmed cell death or apoptosis has been known for some time to play a fundamental role in morphogenetic changes in developing animals, like the sculpting of the developing vertebrate limb (Saunders and Fallon, 1966; Hurle et al., 1996). In *Drosophila,* apoptosis is ultrastructurally and biochemically similar to apoptosis in mammals (White and Steller, 1995), and is required for normal morphogenesis in embryos, particularly in the head region (Nassif et al., 1998). Induction of most of the embryonic apoptosis in *Drosophila* is dependent on three cell death promoting genes, *reaper* (*rpr*) (White et al., 1994), *head involution defective* (*hid*) (Grether et al., 1995), and *grim* (Chen et al., 1996).

The *rpr*, *hid*, and *grim* genes are localized in a small genomic region at 75C, defined by the *Df(3L)H99* deletion (White et al., 1994). Embryos homozygous for this deletion undergo almost no programmed cell death and die prematurely with many additional cells (White et al., 1994). These genes are expressed in transcriptional patterns that presage patterns of embryonic programmed cell death (White et al., 1994; Grether et al., 1995; Chen et al., 1996), although some of the *hid* expressing cells fail to undergo apoptosis (Grether et al., 1995). In addition, their expression is sufficient to initiate apoptosis in some cells, since individual overexpression of any one of these genes results in the death of many cells that would normally live (White et al., 1994; Grether et al., 1995; Chen et al., 1996). Recently, a new *Drosophila* member of the *rpr/hid/grim* gene family at 75C has been identified, called *sickle*, which is also implicated in the activation of apoptosis in embryos (Srinivasula et al., 2002; Wing et al., 2002; Christich et al., 2002). The protein products of the *rpr*, *hid*, *grim*, and *sickle* genes share a short stretch of conserved amino acids at their N terminus (Chen et al., 1996), an IAP binding motif, which is also shared by the mammalian apoptotic proteins SMAC/Diablo and HtrA2/Omi (Du et al., 2000; Verhagen et al., 2000; Suzuki et al., 2001). *Drosophila* Rpr, Hid, Grim, and Sickle proteins independently and combinatorially activate caspase-dependent pathways, at least in part by binding to and inactivating inhibitor of apoptosis proteins (IAPs) (Wang et al., 1999; Goyal et al., 2000; Srinivasula et al., 2002; Wing et al., 2002; Christich et al., 2002). During embryogenesis, the *Drosophila* apoptosis inhibitor DIAP1 seems to be primarily necessary to regulate the death response, as *diap1* null mutants die early in their development due to extensive cell death (Hay et al., 1995). Since the expression patterns of *rpr*, *hid*, *grim*, and *sickle* are distinct and complex with some doomed cells only expressing a subset of these genes, their transcription must be regulated by a variety of inputs, which include cell-cell communication and DNA damage response pathways (Asano et al., 1996; Kurada and White, 1998; Brodsky et al., 2000; Jiang et al., 2000). For example, *hid* expression is negatively regulated by the Ras/MAPK pathway (Kurada and White, 1998), whereas both the p53 and Ecdysone Receptor transcription factors are known to directly activate *rpr* in developing fly cells (Brodsky et al., 2000; Jiang et al., 2000). Thus, *rpr*, *hid*, *grim*, and *sickle* seem to integrate diverse death-inducing signals and relay them to the core death program.

The *Hox* gene *Dfd* is expressed in the maxillary and mandibular segments and necessary for the morphological specializations (mouth hooks, cirri, and ventral organ) of these head segments (McGinnis et al., 1990). In this paper, we demonstrate that in the head of *Drosophila* embryos the Hox protein Dfd directly activates the *rpr* transcription unit, and thereby apoptosis, which is required for the maintenance of a normal boundary be-

[1]Correspondence: wmcginnis@ucsd.edu

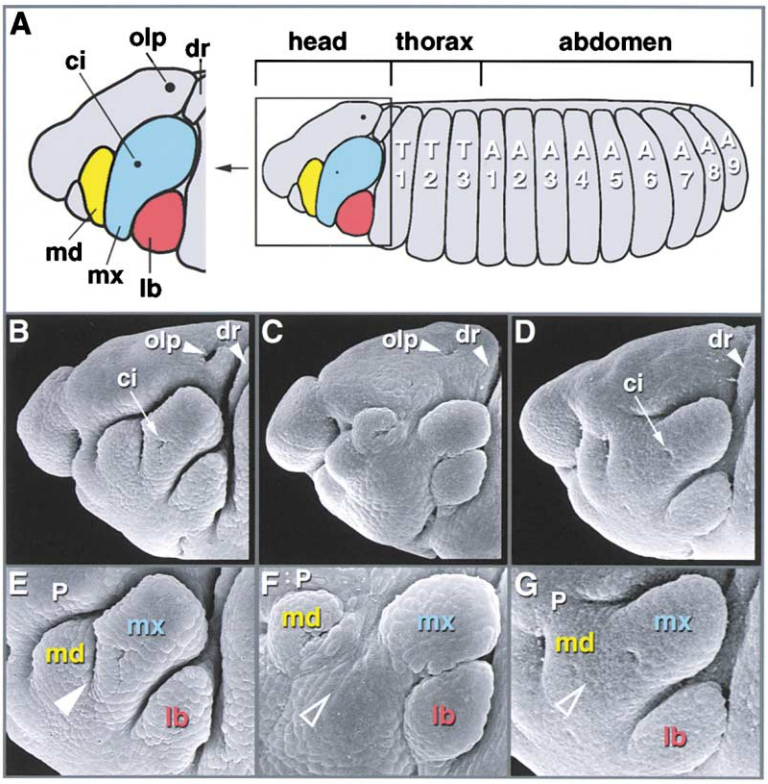

Figure 1. Loss of Apoptosis Mimics Defects in *Dfd* Mutant Embryos

(A) Diagram of a stage 12 wild-type embryo and close-up of the head. Dorsal ridge (dr), optic lobe primordium (olp), maxillary cirri primordium (ci) and gnathal segments, mandibular (md), maxillary (mx), and labial (lb) segments are indicated in this and other images.

(B and E) Scanning electron micrograph of the head of a stage 12 wild-type embryo. (E) A close-up of the gnathal segments shown in (B). The arrowhead marks the boundary between the mandibular and maxillary segments.

(C and F) Head of a stage 12 Dfd^{w21}/Dfd^{r11} mutant. The maxillary cirri primordium and the anterior boundary of the dorsal ridge are missing. The open arrowhead in (F) indicates the missing boundary between the mandibular and maxillary segments.

(D and G) Head of a mutant homozygous for *Df(3L)H99* at stage 12. Arrows in (D) mark the positions where the maxillary cirri primordium and the dorsal ridge would normally develop; the optic lobe primordium is missing. The open arrowhead in (G) indicates the missing boundary between the mandibular and maxillary segments.

P in (E, F, and G) marks the procephalic lobe.

tween the maxillary and mandibular lobes. Our data show a direct link between the *Hox* axial patterning system and a gene that mediates cellular properties underlying a morphological change, a *Hox* realizator gene in the sense of Garcia-Bellido (1977). Moreover, our data and that of others suggest that *Hox* genes may often be required to establish or maintain segment boundaries, in addition to their well-characterized function in the morphological diversification of different segments.

Results

Phenotypic Similarities between *Dfd* Mutants and Cell Death Mutants

To explore the roles of possible downstream effectors of *Dfd* in the maxillary/mandibular segments, we used scanning electron microscopy to analyze the embryonic head morphology of a variety of mutants and compared these to the defects observed in *Dfd* mutants. Stage 12 *Dfd* null mutants had abnormalities in the shape and the location of the mandibular and maxillary lobes, partly due to an apparent excess of cells in the ventral part of the maxillary and mandibular segments (Figure 1C). Strikingly, *Dfd* mutants at this stage were also missing the segment boundary between the maxillary and mandibular segments (Figures 1C and 1F).

The apparent excess of cells located in the ventral maxillary segment in *Dfd* mutants prompted us to focus on mutants in potential downstream genes involved in cell proliferation or cell death. One such mutant, *Df(3L)H99*, which is deleted for the cell death genes *rpr*, *hid*, and *grim*, lacks most of the normal patterns of programmed cell death (White et al., 1994) and has a phenotype that is similar to *Dfd* mutants. Embryos homozygous for the *Df(3L)H99* deficiency have an excess of cells in the ventral and ventrolateral head (Nassif et al., 1998) and are missing the segment boundary between the maxillary and mandibular lobes (Figures 1D and 1G). The similarities in the boundary phenotype between *Dfd* and *Df(3L)H99* mutants suggested that apoptosis might be a morphogenetic process regulated by *Dfd*. Consistent with this line of evidence, we found that the expression of Dfd protein in *Df(3L)H99* homozygous mutants was the same as in wild-type embryos (data not shown), showing that *Dfd* is acting upstream of, and/or in parallel to, genes regulating the apoptosis pathway. The maxillary/mandibular segment fusions were seen beginning at stage 12 in *Dfd* mutant and *Df(3L)H99* mutant embryos, while younger embryos had grossly normal boundaries. Thus, it seems that apoptosis is necessary for the maintenance of this segment boundary, not for its establishment.

Induction of Apoptosis by *Dfd*

To study the role of *Dfd* in the regulation of apoptosis, we analyzed patterns of cell death in wild-type embryos, in *Dfd* mutant embryos, and in embryos that ectopically expressed *Dfd*. In wild-type embryos, the pattern of cellular apoptosis is dynamic, but extensive cell death occurs at maxillary segment boundaries (Nassif et al., 1998). For example, in stage 11 embryos, a cluster of apoptotic cells could be detected at the ventral anterior border of the maxillary segment (Figures 2A and 2B), as visualized by staining with the vital dye Acridine Orange

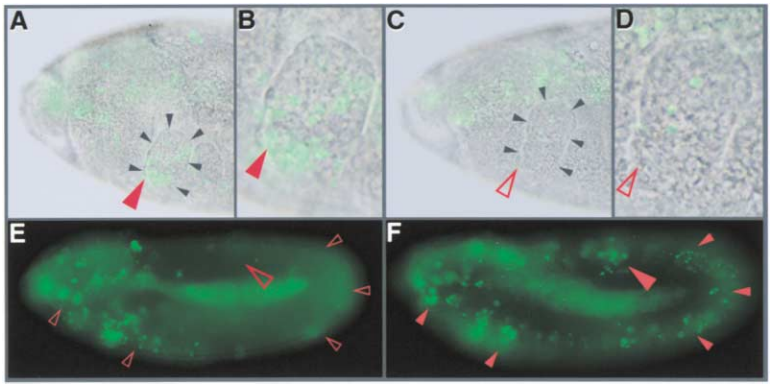

Figure 2. *Dfd* Is Required and Necessary for the Activation of Cell Death

In (A), (B), (C), and (D) brightfield and fluorescent images of Acridine Orange (AO) stainings have been overlaid to reveal the location of AO positive cells.

(A and B) In stage 11 wild-type embryos, many cells undergo apoptosis in the maxillary segment, as visualized by the AO staining. The small black arrowheads in (A) outline the boundary of the maxillary segment. The red arrowheads in (A) and (B) mark the ventrolateral region of the maxillary segment, where cells are dying at the boundary between the maxillary and mandibular segments.

(C and D) In the maxillary segment of a stage 11 *Dfd* (Dfd^{w21}/Dfd^{r11}) mutant, almost no programmed cell death occurs. Note the lack of AO positive cells in the ventrolateral position of the maxillary segment (red, open arrowheads). Closed arrowheads in (C) outline the boundary of the maxillary segment.

(E) In a stage 11 embryo, most apoptosis occurs in the embryonic head of the embryo, almost no cell death in the abdomen (red, open arrowheads).

(F) Ectopic cell death is induced by the overexpression of *Dfd* in a stage 11 *arm*-GAL4::UAS-*Dfd* embryo. Additional apoptotic cells are found both in the embryonic head and the abdomen as measured by AO staining (red arrowheads).

(AO) (Abrams et al., 1993). To test whether apoptotic events in the maxillary segment were dependent on *Dfd*, we examined *Dfd* mutants for the presence of dying cells. In such embryos, the number of apoptotic cells in the maxillary segment was reduced when compared to wild-type embryos (Figures 2C and 2D), demonstrating that Dfd function is required for the activation of cell death in this region. Strikingly, the number of AO positive cells along the maxillary/mandibular border was significantly reduced (Figures 2C and 2D). To analyze whether *Dfd* is sufficient to activate cell death, we ectopically expressed *Dfd* using the UAS-GAL4 system (Brand and Perrimon, 1993). When *Dfd* is driven ubiquitously by *armadillo* (*arm*)-GAL4 (Sanson et al., 1996), the number of apoptotic cells increased substantially in embryonic head and abdominal segments (Figure 2F).

As *Dfd* expression is sufficient to activate apoptosis in embryos, it may be able to do so in other tissues. To test this possibility, we used the GMR-GAL4 driver to ectopically express *Dfd* in cells of the developing *Drosophila* eye (Hay et al., 1997). When we ectopically expressed a single copy of *Dfd* in the developing eye, a mild eye ablation phenotype resulted (Figure 3B). A dramatically rough appearance and a severe reduction in the eye size were observed when a constitutively active form of *Dfd*, *Dfd-VP16* (Li et al., 1999), was expressed in the eye primordium (Figure 3C). As a positive control, we misexpressed *rpr* in the developing eye, which nearly eliminated the adult eye (Figure 3D).

Using this assay, we wanted to confirm that *Dfd* induces cell death through the activation of well-characterized programmed cell death pathways. To this end, we coexpressed Dfd or Dfd-VP16 in the developing eye with the anti-apoptotic protein DIAP1, which functions to block cell death by binding to and inactivating the caspase family of proteases (Wang et al., 1999). In these experiments, *Dfd* overexpression phenotypes were suppressed (Figures 3F and 3G), with eye size and appearance being similar to the control expressing GMR-*DIAP1* alone (Figure 3E). Coexpression of DIAP1 with Dfd-VP16 partially rescued the eye ablation phenotype, although the eyes were still relatively small and rough in their appearance (Figure 3G). As expected, expression of DIAP1 provided a strong rescue of the eye ablation phenotype caused by ectopic GMR-*rpr* (Figure 3H). Since DIAP1 specifically functions to antagonize caspase-dependent apoptosis (Hay et al., 1995; Wang et al., 1999), these experiments showed that Dfd and Dfd-VP16 are able to activate cell death through the activation of a caspase-dependent pathway.

Regulation of the Cell Death Promoting Gene *rpr* by Dfd

As the genomic region containing *rpr*, *hid*, and *grim* is required for most apoptotic cell death in *Drosophila* embryos (White et al., 1994), we tested whether *Dfd* activated one or more of these genes in the maxillary segment. All three genes are expressed in cells of the maxillary segment in wild-type embryos (data not shown), although only *rpr* was strongly expressed at the boundary between the maxillary and mandibular segments (Figures 4B and 4C), the boundary missing in *Dfd* mutant embryos (Figures 1C and 1F). Strikingly, this transcriptional domain of *rpr* was nearly eliminated in *Dfd* mutants (Figures 4E and 4F), while other domains of *rpr* expression in the maxillary segment, e.g., at the boundary to the labial segment, were unchanged (Figures 4E and 4F). Since the expression of *grim* and *hid* was unaffected in *Dfd* mutants (data not shown), this result demonstrated that at the boundary between the maxillary and mandibular lobes, *rpr* transcription is dependent on *Dfd* function.

To test whether *Dfd* is also sufficient to induce the transcription of *rpr*, we ectopically expressed the UAS-*Dfd* transgene (Li et al., 1999) using the *paired (prd)*-GAL4 driver (Yoffe et al., 1995). In *prd*-GAL4::UAS-*Dfd* embryos, *rpr* was expressed in a *paired*-like pattern (Figures 4H and 4I), overlapping with the ectopic expression pattern of Dfd protein (Figure 4G). The same result was obtained when misexpressing the UAS-*Dfd-VP16* transgene (Li et al., 1999) using the *prd*-GAL4 driver, although the activation of *rpr* was much stronger (data

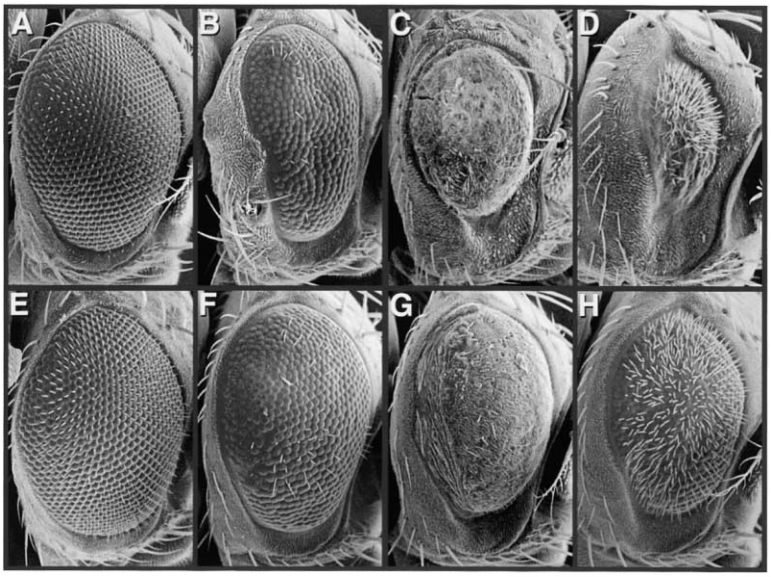

Figure 3. Expression of *DIAP1* Suppresses *Dfd*- or *Dfd-VP16*-Dependent Death in the Eye

Scanning electron micrographs of adult compound eyes. The following genotypes are shown: (A) GMR-GAL4/+; (B) GMR-GAL4::UAS-*Dfd*; (C) GMR-GAL4::UAS-*DfdVP16*; (D) GMR-*rpr*/+; (E) GMR-GAL4, GMR-*DIAP1*/+; (F) GMR-GAL4, GMR-*DIAP1*::UAS-*Dfd*; (G) GMR-GAL4, GMR-*DIAP1*::UAS-*DfdVP16*; (H) GMR-Gal4, GMR-*DIAP1*; GMR-*rpr*. As a positive cell death control, the consequences of targeted *rpr* expression in the developing eye is shown, which results in a small eye phenotype (D). The cell death induced reduction in the eye size by *Dfd* (B), *Dfd-VP16* (C) or *rpr* (D) can be prevented by coexpression of the *Drosophila* apoptosis inhibitor *DIAP1* (F, G, and H).

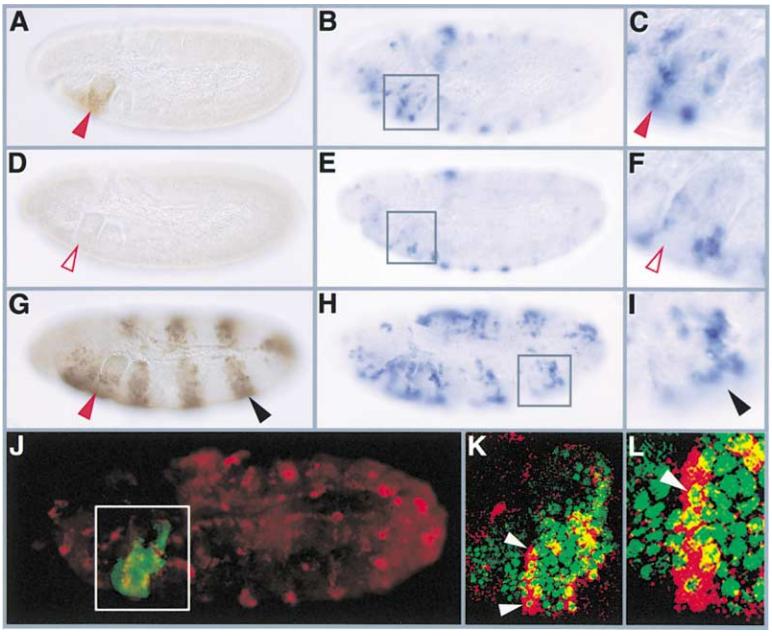

Figure 4. Activation of *rpr* in the Maxillary Segment Is Dependent on Dfd

(A, D, and G) Dfd antibody staining of a stage 11 wild-type embryo (A), Dfd^{w21}/Dfd^{r11} mutant embryo (D) and an embryo ectopically expressing *Dfd* using the *prd*-GAL4 driver (G). The red closed (A and G) and open (D) arrowheads mark the anterior border of the maxillary segment. The black arrowhead in (G) marks an additional stripe of Dfd expression in the A3 primordium.

(B and C) *rpr* RNA expression in a stage 11 wild-type embryo. The box in (B) outlines the maxillary segment. (C) shows a close-up of the maxillary segment in (B). *rpr* is strongly expressed at the boundary between the maxillary and mandibular segment (marked by the red arrowhead).

(E and F) In a stage 11 Dfd^{w21}/Dfd^{r11} mutant embryo, *rpr* expression is dramatically reduced at the boundary between the maxillary and the mandibular lobes (highlighted by red, open arrowhead), otherwise the expression is unchanged. The box in (E) outlines the maxillary segment, a close-up of which is shown in (F).

(H and I) *rpr* RNA expression in an embryo ectopically expressing *Dfd* using the *prd*-GAL4 driver. *rpr* is strongly induced in the areas where Dfd protein is present. The box outlines an additional stripe of *rpr* RNA expression in the A3 primordium.

(J) Double-labeling of Dfd protein and *rpr* RNA in a stage 11 wild-type embryo. The box marks the maxillary segment, where Dfd protein and *rpr* RNA colocalize. The apparent differences in abdominal *rpr* expression pattern between Figure 4B and 4J are due to different focal planes.

(K and L) Confocal image of the maxillary segment of the embryo shown in (J). Dfd protein and *rpr* RNA colocalize in anterior maxillary cells, although Dfd is also present in areas where no *rpr* transcripts can be detected. The arrowheads in (K) mark the boundary between the maxillary and mandibular segments. (L) A close-up of the boundary between the maxillary and mandibular segments is shown in (K). The arrowhead marks a nucleus with Dfd protein, which is surrounded by cytoplasm containing *rpr* RNA.

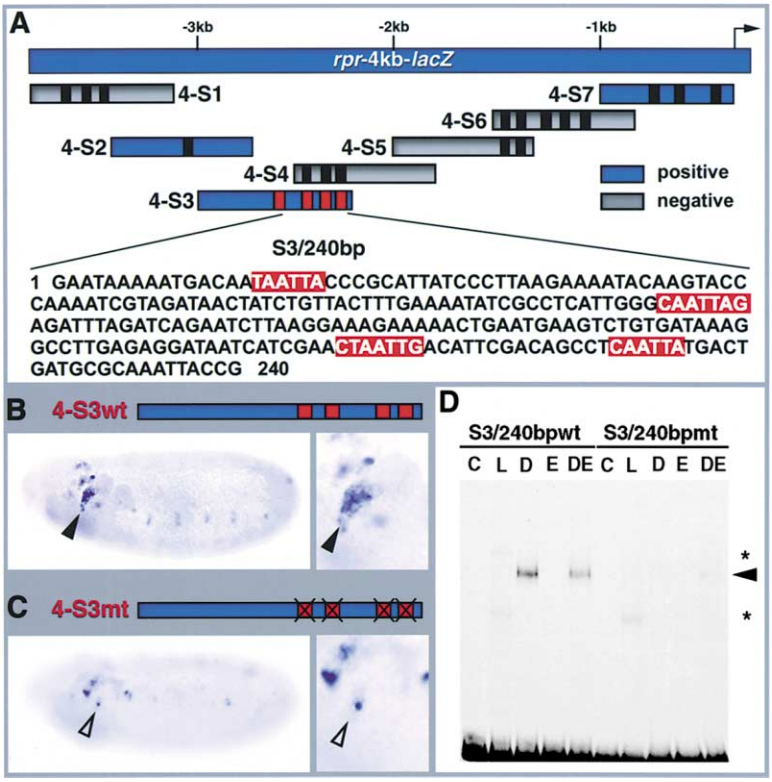

Figure 5. Dfd Binding Sites Are Required for *rpr* Enhancer Activity in *Drosophila* Embryos

(A) Top: diagram of *rpr-lacZ* reporter lines tested. Each fragment, depicted as bars, was fused to a *lacZ* reporter gene including a *hsp70* minimal promoter. 4-S1 to 4-S7 represent subfragments of the *rpr*-4kb-*lacZ* reporter. Reporter lines were considered positive, when they showed expression in the maxillary segment. Putative Dfd binding sites are indicated in each fragment by vertical bars. Bottom: sequence of the 3′ end of the 4-S3 fragment is shown on the bottom, with the Dfd binding sites highlighted in red. This fragment, S3/240bp, was used in the electrophoretic mobility shift assay shown in (D).

(B) β-galactosidase is expressed strongly at the boundary between the maxillary and mandibular segments in the 4-S3 wt reporter (wild-type Dfd binding sites). This resembles some aspects of the *rpr* wild-type expression in the maxillary segment (Figures 4B and 4C).

(C) In the 4-S3 mt reporter, with all four Dfd binding sites mutated, the expression of *lacZ* is dramatically reduced in the anterior part of the maxillary segment of early stage 11 embryos when compared to the 4-S3 wt reporter.

(D) EMSA using the S3/240 bp fragment (A) and no protein (C), translation lysate only (L), lysate with Dfd protein (D), lysate with Exd protein (E), and lysate with both Dfd and Exd (DE). The black arrowhead indicates the specific DNA-protein complex containing Dfd protein. Asterisks indicate complexes with lysate proteins seen also in the control.

not shown). Together these results are compatible with the notion that *Dfd*, directly or indirectly, activates *rpr* transcription. Furthermore, when performing a double label experiment, *rpr* transcripts and Dfd protein colocalized in many cells of the maxillary segment (Figures 4J, 4K, and 4L). In sum, the requirement of Dfd for *rpr* expression in anterior maxillary cells, along with the colocalization of *rpr* RNA and Dfd protein in those cells, suggested that Dfd might directly regulate *rpr* transcription.

Direct Regulation of *rpr* by Dfd

We next addressed whether the regulation of *rpr* transcription by *Dfd* is direct or indirect. To map *Dfd*-responsive sequences in the *rpr* enhancer, we examined the activity of existing *rpr-lacZ* reporter lines (Brodsky et al., 2000; Jiang et al., 2000). All the lines were analyzed for their ability to activate *lacZ* transcription in cells of the maxillary segment that normally express *rpr*. The *rpr*-4kb-*lacZ* transgenic line, carrying a 4 kb fragment upstream of the *rpr* transcription start (Jiang et al., 2000), showed an overall *lacZ* expression resembling endogenous *rpr*. This reporter was activated in cells of the maxillary segment, including some cells located at the boundary between the maxillary and the mandibular segments (data not shown). We tested smaller fragments of this 4 kb regulatory region for their ability to activate *lacZ* transcription at the maxillary/mandibular border (Figure 5A). Three reporter constructs, 4-S2, 4-S3, and 4-S7 respectively, directed *lacZ* expression in the maxillary segment (Figure 5A). One of these, a 674 bp fragment named 4-S3, strongly activated reporter expression at the maxillary/mandibular boundary, as well as in few additional maxillary and procephalic cells (Figure 5B). Strikingly, a cluster of four matches to Dfd consensus binding sites is located at the 3′ end of the 4-S3 fragment (shown in Figure 5A, S3/240bp). Using electrophoretic mobility shift assays (EMSA), we found that Dfd binds to this fragment (S3/240bpwt; Figure 5D). The Exd protein, which often acts as a cooperatively binding Hox cofactor (Mann and Affolter, 1998), did not enhance the binding affinity of Dfd for this fragment, but instead reduced Dfd binding. When the four Dfd consensus binding sites were mutated (S3/240bpmt), binding of Dfd to this fragment was almost completely abolished (Figure 5D).

We next tested the importance of the Dfd binding sites in vivo by mutating the sites in the 4-S3 reporter. As shown in Figure 5C, the mutated element (4-S3 mt) largely lost its ability to drive reporter gene expression in the anterior maxillary segment of early stage 11 embryos, suggesting that the Dfd binding sites are necessary for activity of this *rpr* enhancer in vivo. A similar lack of maxillary reporter expression was observed when we analyzed the expression of the wild-type element (4-S3 wt) in a *Dfd* mutant background (data not shown). Finally, we tested the activity of the 4-S3 wt element in embryos overexpressing Dfd, and found that 4-S3 wt could be ectopically induced in the gnathal region and the anterior

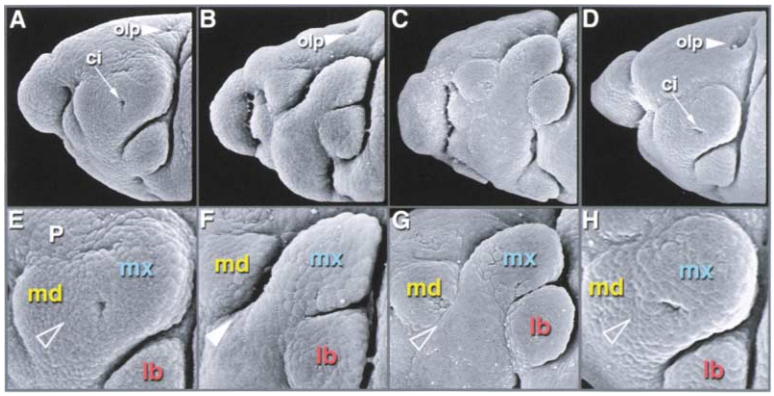

Figure 6. Apoptosis and *rpr* Expression Are Required for the Maintenance of the Boundary between the Maxillary and Mandibular Segments

In all images, the maxillary cirri primordium (ci), the optic lobe primordium (olp), the procephalic lobe (P), the mandibular (md), the maxillary (mx), and the labial segment (lb) are marked.

(A and E) Scanning electron micrographs of the head of a stage 12 UAS-*DIAP1*::*wg*-GAL4 embryo. The *wg*-GAL4 driver contains 7.8 kb of 5′ untranslated control region of the *wg* gene providing all functions for its embryonic expression pattern, including the anterior region of the maxillary segment (Schmidt-Ott and Technau, 1992). In a magnification of the gnathal segments of the embryonic head (E), the open arrowhead marks the missing boundary between the mandibular (md) and maxillary (mx) segments.

(B and F) In a stage 12 Dfd^{w21}/Dfd^{r11} mutant embryo, the *Dfd*-dependent boundary defect is rescued by expressing *rpr* at the border between the maxillary (mx) and mandibular (md) segments using the *wg*-GAL4 driver. In (F), the closed arrowhead marks the cleft, resembling a segment boundary.

(C and G) The head of a stage 12 Dfd^{w21}/Dfd^{r11}; *wg*-GAL4 control embryo. The open arrowhead marks the missing boundary between the maxillary and mandibular segments normally seen in *Dfd* mutants.

(D and H) In a stage 12 *XR38*/*H99* mutant embryo, which is deleted for the *rpr* gene, the maxillary/mandibular boundary is missing (marked by open arrowhead). In (H), a magnification of the gnathal segments of the embryonic head in (B) is shown.

part of all the trunk segments in *arm*-GAL4::UAS-*Dfd* embryos (data not shown).

Rescue of the *Dfd* Mutant Boundary Defect by Induction of Localized Apoptosis

Although the *Df(3L)H99* deletion eliminates the *rpr*, *hid*, and *grim* genes, it spans an interval of ~300 kb (White et al., 1994), so it was still possible that the segment boundary phenotype (Figures 1D and 1G) was due to the deletion of another gene in the *Df(3L)H99* region. As an additional test of whether programmed cell death per se is required for segmental border maintenance, we ectopically expressed the apoptosis inhibitor *DIAP1* using the *wg*-GAL4 driver. This driver provides expression in a segmental pattern, and in the maxillary segment its expression is limited to the anterior region of the segment (Schmidt-Ott and Technau, 1992). Since DIAP1 is sufficient to block most programmed cell death in the embryo (Hay et al., 1995), its expression in cells at maxillary/mandibular boundary should result in border loss if apoptosis is necessary for the border to be maintained. Consistent with our previous results, the segment boundary between the maxillary and mandibular segments was abolished in UAS-*DIAP1*::*wg*-GAL4 embryos (Figures 6A and 6E), indicating that programmed cell death is necessary for its maintenance. In addition, we observed a fusion of the mandibular with the procephalic segment (Figure 6E), again similar to the phenotype seen in *Df(3L)H99* homozygous mutants (Figure 1G), suggesting that the maintenance of this segmental border is also dependent on the activity of *rpr*, *hid*, or *grim*.

We also wished to test whether *rpr* expression is sufficient for the maintenance of the border between the maxillary and mandibular lobes, when *rpr* is activated at the boundary in a manner independent of Dfd. Therefore, the *wg*-GAL4 driver was used to direct the expression of *rpr* (data not shown) in the anterior region of the maxillary segment in a *Dfd* mutant background. This resulted in a reversion of the boundary loss seen in *Dfd* mutant embryos (Figures 6C and 6G), as a cleft not normally present in *Dfd* mutants was formed between the two head lobes, resembling the phenotype of wild-type embryos (Figures 6B and 6F, compare with Figures 1B and 1E). Finally, we tested whether *rpr* function alone is necessary for maxillary/mandibular boundary maintenance. Peterson et al. (2002) defined a deletion, *XR38*, that, in transheterozygous combination with the *Df(3L)H99* deletion, eliminates only the *rpr* gene. In these mutant embryos, the boundary between the maxillary and mandibular segments was largely abolished (Figures 6D and 6H). Thus, we concluded that normal *rpr* function is required to maintain the maxillary/mandibular boundary, and is sufficient, perhaps in combination with other apoptosis promoting genes, to induce the boundary when *Dfd* function is removed.

Regulation of Localized Apoptosis and Segment Boundaries by Another *Hox* Gene

We were intrigued by the possibility that other *Hox* genes might also use control of apoptosis to establish or maintain segmental borders along the A/P axis. Therefore, we examined one other *Hox* gene, *Abd-B*, which is required for the proper development of abdominal segments A6 to A9 (Sanchez-Herrero et al., 1985). In late stage 12 wild-type embryos, the boundaries between segments A6 to A9 are clearly formed with deep clefts between the individual segments (Figures 7A and 7D). In contrast, in $Abd\text{-}B^{M}$ mutants ($Abd\text{-}B^{M5}/Df(3R)P115$), which do not express Abd-B in parasegments 10 to 13 (Delorenzi and Bienz, 1990), the boundaries between segments A6 and A7 and between A7 and A8 were partially fused (Figures 7B and 7E). As the same phenotype was observed in the *Df(3L)H99* deficiency line (Figures 7C and 7F), we considered the possibility that Abd-B also regulates apoptosis and the activation of *rpr* to maintain normal segment boundaries. Consistent with this model, *rpr* transcripts were expressed in a portion of the border of posterior segments in wild-type embryos (Figures 7G and 7H), while this expression was absent

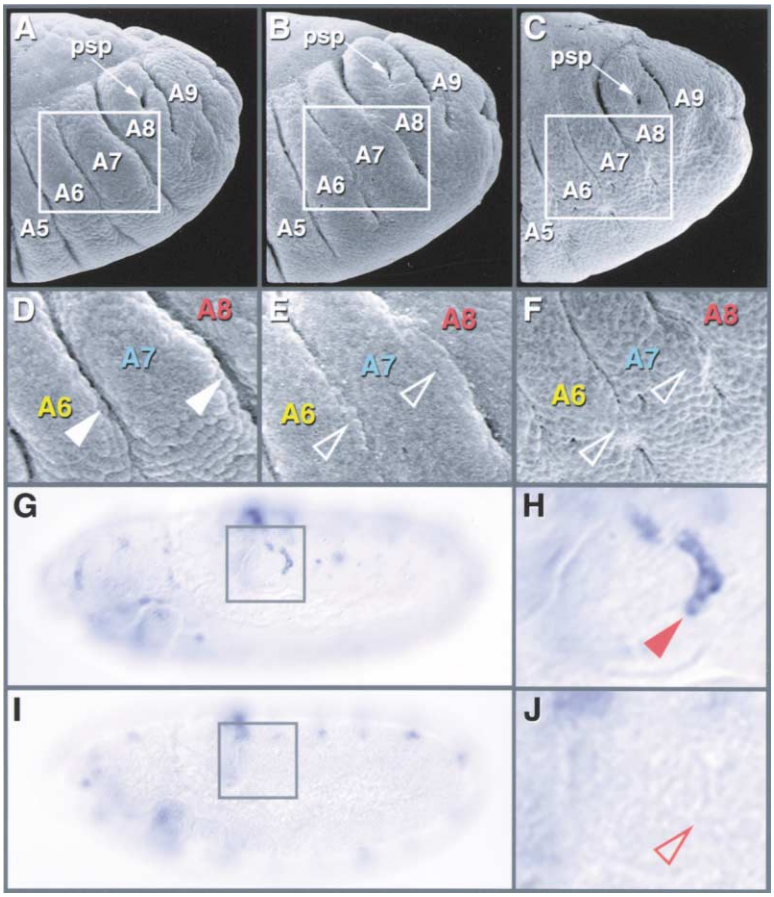

Figure 7. *Abd-B* Regulates Segment Boundary Formation in the Posterior Region Via Apoptosis

(A and D) Scanning electron micrographs of the posterior segments A5 to A9 in a wild-type embryo. In (D), a magnification of segments A6 to A8 is shown. Arrowheads in (D) mark the A6/A7 and the A7/A8 boundaries.

(B and E) Posterior segments of a stage 12 *Abd-B*^{M5}/*Df(3R)P115* transheterozygous mutant. In (E), the open arrowhead indicates the partially fused boundaries between segments A6/A7 and A7/A8.

(C and F) Segments A5 to A9 of a stage 12 mutant homozygous for *Df(3L)H99*. The fused segment boundaries are marked by open arrowheads in (F).

Arrows in (A), (B), and (C) mark the posterior spiracle primordium (psp) in segment A8.

(G and H) *rpr* RNA is expressed at the A8/A7 boundary (marked by the red arrowhead). *rpr* is also expressed at the A7/A6 boundary (out of focus). The box in (G) outlines the abdominal segment A8, a close-up of which is shown in (H).

(I and J) In a stage 11 *Abd-B*^{M5}/*Df(3R)P115* transheterozygous mutant, *rpr* expression at the A8/A7 boundary (and also at the A7/A6 boundary) is missing. A close-up of segment A8, marked by a box in (I), is shown in (J).

at the segmental borders A6/A7 and A7/A8 in *Abd-B*^{M5}/*Df(3R)P115* mutants (Figures 7I and 7J). Furthermore, *rpr* expression was ectopically activated in *prd*-GAL4::UAS-*Abd-B* embryos (data not shown). Like Dfd, Abd-B is also capable of activating apoptosis, since its expression in the developing eye resulted in a severe reduction of eye size, a phenotype that was partially suppressed by the coexpression of DIAP1 or p35 (data not shown). In sum, these experiments indicated that not only *Dfd*, but also *Abd-B,* activates an apoptosis-promoting gene and uses programmed cell death as a realizator process for maintaining normal segment boundaries.

Discussion

Several lines of evidence—the effects of manipulating *rpr* expression in embryos, in vitro DNA binding studies with Dfd protein and mutagenesis of Dfd binding sites in the *rpr* enhancer, the phenocopy of the *Dfd* mutant boundary defect with an apoptosis inhibitory gene, its rescue with an apoptosis promoting gene, and the phenotype of *rpr* mutants—show that the Hox protein Dfd is a direct transcriptional activator of *rpr* in the anterior maxillary segment, and that *rpr* expression and apoptosis are necessary to maintain the maxillary/mandibular boundary. At least in part, this Dfd-dependent, anterior maxillary expression of *rpr* is conferred by a 674 bp enhancer (*rpr* 4-S3) that maps 3.1 kb upstream of the *rpr* transcription start. This demonstrates that a Hox protein directly regulates a cell biological effector gene that mediates a morphological subroutine for that Hox function. Therefore, *rpr* qualifies as a directly regulated realizator gene in the sense of Garcia-Bellido (1977). Interestingly, although Dfd is expressed in nearly all maxillary cells, the loss of Dfd function did not influence *rpr* expression in the posterior maxillary segment, indi-

Table 1. Frequencies of Mutant and Overexpression Phenotypes

Figure	Genotype	Wild-type phenotype	Mutant or misexpression phenotype	% Mutant and/or misexpression phenotype
1	*Dfd*^{w21}/*Dfd*^{r11}	52	14	21
1	*Df(3L)H99*	56	16	22
6	*XR38/Df(3L)H99*	60	19	24
6	*Dfd*^{w21}/*Dfd*^{r11}; *wg::rpr*	46	12 (plus 2 *Dfd*$^{-}$)	26
6	*wg::DIAP1*	23	90	80
7	*Abd-B*^{M5}/*Df(3R)P115*	52	18	26
7	*Df(3L)H99*	68	20	23

cating that other activators and/or repressors of *rpr* are distributed in maxillary cells that influence the transcriptional activity of Dfd protein on this locus. In the tail region, we showed that *Abd-B* is also required for the formation of normal boundaries between the abdominal segments A6/A7 and A7/A8, and that their maintenance correlates, as in the case of the maxillary/mandibular boundary, with the localized activation of *rpr*. Thus, at both termini of the *Drosophila* body, Hox control of apoptosis is used for segment boundary maintenance.

Hox proteins may have a wider role in the programming of segmental boundaries than is currently believed. There is strong evidence that two *Drosophila* homeobox genes that are used to control segment number, *even-skipped* and *fushi-tarazu*, are independently derived from genes that still possess Hox segment identity functions in most insects and other arthropods (Dawes et al., 1994; Brown et al., 1994; Patel, 1994; Telford, 2000; Lohr et al., 2001; Hughes and Kaufman, 2002). In addition, mutants in the mouse *Hoxa-2* gene have segmentation defects in the hindbrain (Gavalas et al., 1997). Although a segmental boundary is normally established between rhombomeres 1 and 2 in the *Hoxa-2* mutants, it is not maintained, which is reminiscent of the defect in boundary maintenance we observe in *Dfd* mutant embryos.

Surprisingly, although we have shown that *rpr* is required for maxillary/mandibular boundary maintenance during embryogenesis, flies lacking *rpr* function survive to adulthood with only minor defects (Peterson et al., 2002). One possible explanation is that other cell death activators can compensate for the absence of *rpr* at later stages of development, since other apoptosis genes, like *hid*, *grim*, and *sickle*, are expressed in overlapping patterns with *rpr* and share IAP binding motifs in their N-terminal protein sequence (Chen et al., 1996; Srinivasula et al., 2002; Wing et al., 2002; Christich et al., 2002). This may also explain why the maxillary/mandibular segmentation defect is less severe in *Dfd* null mutants and in *XR38/H99* mutants (Figures 1C and 1F and Figures 6C and 6F) when compared to homozygous *Df(3L)H99* mutants (Figures 1D and 1G). Since *rpr* and *hid*, but not *grim*, are expressed in anterior maxillary cells at many developmental stages, and since the combined activities of *hid* and *rpr* dictate the probability of a cell to undergo apoptosis (Kurada and White, 1998), we suggest that in wild-type embryos the combination of *rpr* and *hid* are required to kill cells at the maxillary/mandibular boundary.

Many *Drosophila* genes are known to be regulated in a Hox-dependent manner, but most encode either transcriptional regulators or cell signaling molecules (Graba et al., 1997; Pradel and White, 1998). These *Hox* effectors presumably act both independently and/or in parallel to *Hox* genes to indirectly influence cell type identity and morphology. For example, the Hox target gene *Distal-less* (*Dll*) is required for the development of embryonic appendages and is directly repressed in abdominal segments by the Hox proteins Ubx and Abd-A (Vachon et al., 1992). However, at some point the Hox proteins, their downstream effectors, and other cofactors must affect cellular changes by means of the class of realizator genes originally postulated by Garcia-Bellido (1977).

There are three good candidates for realizator genes in *Drosophila*, *connectin*, *centrosomin*, and β-*tubulin*. *connectin* encodes an extracellular cell surface protein with leucine-rich repeats. It mediates cell-cell adhesion in cell culture assays (Meadows et al., 1994) and acts as a homophilic cell adhesion molecule in the lateral transverse muscles (Raghavan and White, 1997). In the nervous system, *connectin* expression is under the control of *Ubx* (Gould and White, 1992), and a small regulatory fragment that mediates portions of its expression was isolated by its affinity for Ubx in coimmunoprecitation assays. In some tissues, *connectin* is under the direct control of Ubx protein, but it is still unclear which of the morphogenetic subfunctions of *Ubx* require *connectin* function. *centrosomin* is a subunit of the centrosome and is necessary for the proper development of the CNS, PNS, and midgut (Heuer et al., 1995; Li and Kaufman, 1996). During the formation of the second midgut constriction, the functions of both *Ubx* and *centrosomin* are required, and *centrosomin* is lost in the visceral mesoderm cells of *Ubx* mutants (Heuer et al., 1995). The β-*tubulin* gene encodes a major component of microtubules and contains a *cis*-regulatory element that is regulated by *Ubx* in the visceral mesoderm (Hinz et al., 1992).

We have also shown that in *Drosophila*, as in vertebrates, programmed cell death is used for the sculpting of morphological structures. For example, limb formation in amniotes is accompanied by massive cell death in almost all the interdigital mesenchymal tissue located between the chondrifying digits, eliminating the cells located between the differentiating cartilages and thus sculpting the shape of the limb (Hurle et al., 1996). Interestingly, in *Hoxa13* heterozygous mutant mice, the apoptosis that normally occurs in the interdigital regions is reduced, leading to a partial fusion of digits II and III in adult mice. In *Hoxa13* homozygous mutant mice, there is no interdigital apoptosis and no digit separation in 14-day-old embryos (Stadler et al., 2001). Although it remains to be seen whether *Hoxa13* and other *Hox* genes are direct regulators of apoptotic genes in amniotes and other animals, we are intrigued by the possibility that *Hox*-dependent regulation of apoptosis is a more general mechanism used to generate and maintain metameric pattern during animal development.

Experimental Procedures

Drosophila Genetics

The wild-type strain used was Oregon-R. *Df(3L)H99*, *Df(3R)P115*, GMR-*rpr*, and UAS-*rpr* strains were obtained from the Bloomington Stock Center; *rpr*-4kb-*lacZ* flies from C. Thummel (Jiang et al., 2000); GMR-GAL4, GMR-*DIAP1* flies from P. Meier (Meier et al., 2000); *XR38* flies from K. White (Peterson et al., 2002); UAS-*DIAP1* flies from B. Hay; and the *wg*-GAL4 line homozygous on the second chromosome from E. Bier. Transheterozygous mutants were used by crossing either Dfd^{w21}/TM3*Sb*[*Ubx*::*lacZ*] and Dfd^{r11}/TM3*Sb*[*Ubx*::*lacZ*] or $Abd\text{-}B^{M5}$/TM3*Sb*[*Ubx*::*lacZ*] and *Df(3R)P115*/TM3*Sb*[*Ubx*::*lacZ*] embryos. To identify *Dfd* mutant embryos prior to AO staining, Dfd^{w21} and Dfd^{r11} fly strains were crossed to *D gl*/TM3*Sb*[*Kr*::GFP] (Casso et al., 2000). *Dfd* mutants (Dfd^{w21}/Dfd^{r11}) were identified by the absence of GFP expression in the posterior end of stage 11 embryos. For *rpr* misexpression in *Dfd* mutant embryos, *wg*-GAL4; Dfd^{r11} and UAS-*rpr*; Dfd^{w21} lines were generated by crossing *wg*-GAL4 and Dfd^{w21}/TM3*Sb*[*Ubx*::*lacZ*] lines and UAS-*rpr* and Dfd^{r11}/TM3*Sb*[*Ubx*::*lacZ*] lines, respectively.

Embryonic Phenotypes

Embryos for scanning electron microscopic studies were collected for 3 hr followed by 6 hr of aging at 24°C or 29°C. Even with a short collection window, developmental time was not perfectly correlated with developmental stage, so comparable stages between control and experimental embryos in the table below were scored based on three major factors; location of the gnathal segments relative to the dorsal ridge, location and morphology of the posterior spiracle primordium, and the extent of germ band retraction. Results are shown in Table 1.

Plasmids

To construct *rpr* reporters, *rpr* regulatory regions were amplified from Oregon-R genomic DNA with Expand High-Fidelity polymerase (Roche Molecular Biochemicals, Indianapolis, IN) and primer sets: 4-S1a (ACT AGT CCG AGC ACT ACG GAT CAC) and 4-S1b (CTC GAG GTT TCA GCT TTC TCT CGT TC) for 4-S1; 4-S2a (ACT AGT GTA ATG CAG GGA ATA TAT AGG) and 4-S2b (CTC GAG CAA CGT GAT ATT CCC AAA TG) for 4-S2; 4-S3a (ACT AGT GAG GCA GTC CCA GAC AAA G) and 4-S3b (CTC GAG GTA TGT CCT TCG CGG TAA C) for 4-S3; 4-S4a (ACT AGT GTA GAT AAC TAT CTG TTA CTT TG) and 4-S4b (CTC GAG GCG TGC TCG TTC TCT TTC) for 4-S4; 4-S5a (ACT AGT GTT GTA TGT GTG TGT TGA CGC) and 4-S5b (CTC GAG CCG AAC AAT GTA TTC TTC CAA C) for 4-S5; 4-S6a (ACT AGT GTT TAT GGG TAA TCC GAC TTA G) and 4-S6b (CTC GAG GTA AGG GTA TTA TAA CAA GTG G) for 4-S6; 4-S7a (ACT AGT GAT TGT GTA AAC ACT TGT AGA GC) and 4-S7b (CTC GAG GTT GTG TTG TTG TTG CCA G) for 4-S7. Products were cloned, sequenced, and shuttled into pH-Pelican (Barolo et al., 2000) using 5′ SpeI and 3′ XhoI sites (underlined). For 4-S3mt, the Dfd binding sites, TAATT(A/G) and CAATTA(T/G), were mutated to TCCTT(A/G) and CAAGGA(T/G). All P element constructs were introduced into w^{1118} flies by P element-mediated germline transformation (Rubin and Spradling, 1982).

Histology and Scanning Electron Microscopy

In situ hybridization and immunochemistry were performed as described (Bergson and McGinnis, 1990). The 1A2E9 anti-Abd-B monoclonal antibody was obtained from E.B. Lewis. For fluorescent double labeling of RNA and protein, in situ hybridization was performed first omitting proteinase K treatment. A biotinylated *rpr* RNA probe was used with a streptavidin-HRP coupled secondary antibody (NEN Life Science Products, Boston, MA; used at a 1:300 dilution) and the TSA Tetramethylrhodamine System (NEN Life Science Products, Boston, MA). After washing in PBT, embryos were blocked in PBT + 2% blocking reagent (Roche Molecular Biochemicals, Indianapolis, IN), before overnight incubation with Dfd antibody in PBT + 2% blocking reagent (4°C). After washing, embryos were incubated with FITC-coupled secondary antibody for three hours, washed in PBT, and mounted in FluoroGard Antifade reagent (Roche Molecular Biochemicals, Indianapolis, IN). Analysis was carried out using a Microphot-FXA or PCM 2000 Confocal microscope (Nikon). AO staining was performed as described in Abrams et al. (1993). Flies and embryos were prepared for SEM essentially as described in Kimmel et al. (1990) and in Handel et al. (2000).

Electrophoretic Mobility Shift Assays

Dfd and Exd proteins were expressed by coupled in vitro transcription/translation (Promega) using plasmids pEXD and pDFD. Fragments S3/240bpwt and S3/240bpmt were end-labeled with [γ^{32}P]-ATP using T_4 polynucleotide kinase (NEB, Beverly, MA) before purification over a polyacrylamide gel. The binding reaction, with 50 fmol of target DNA, was incubated for 20 min on ice in 20 mM Tris [pH 7.5], 150 mM NaCl, 0.25 mM EDTA, 20% glycerol, 1 mM dithiothreitol, 20 mM $MgCl_2$ and 1 $\mu g\ \mu l^{-1}$ double-stranded poly(dIdC) (Roche Molecular Biochemicals, Indianapolis, IN). Electrophoresis was carried out at 4°C on a 4% nondenaturing polyacrylamide gel.

Acknowledgments

We thank J. Lohmann, K. Mace, O. Taghli, E. Tour, A. Veraksa, and D. Weigel for reading the manuscript and discussion; E. Bier, B. Hay, E.B. Lewis, C. Thummel, K. White, and the Bloomington Stock Center for material; and D. Kosman for excellent technical help. Supported by the European Molecular Biology Organization (I.L., ALTF-72-1999), the Deutsche Forschungsgemeinschaf (I.L, LO 844/2-1), and the National Institutes of Health (W.M.).

Received: March 28, 2002
Revised: June 21, 2002

References

Abrams, J.M., White, K., Fessler, L.I., and Steller, H. (1993). Programmed cell death during *Drosophila* embryogenesis. Development *117*, 29–43.

Asano, M., Nevins, J.R., and Wharton, R.P. (1996). Ectopic E2F expression induces S phase and apoptosis in *Drosophila* imaginal discs. Genes Dev. *10*, 1422–1432.

Barolo, S., Carver, L.A., and Posakony, J.W. (2000). GFP and β-galactosidase transformation vectors for promoter/enhancer analysis in *Drosophila*. Biotechniques *29*, 726–732.

Bergson, C., and McGinnis, W. (1990). An autoregulatory enhancer element of the *Drosophila* homeotic gene *Deformed*. EMBO J. *9*, 4287–4297.

Brand, A.H., and Perrimon, N. (1993). Targeted gene expression as a means of altering cell fates and generating dominant phenotypes. Development *118*, 401–415.

Brodsky, M.H., Nordstrom, W., Tsang, G., Kwan, E., Rubin, G.M., and Abrams, J.M. (2000). *Drosophila* p53 binds a damage response element at the *reaper* locus. Cell *101*, 103–113.

Brown, S.J., Hilgenfeld, R.B., and Denell, R.E. (1994). The beetle *Tribolium castaneum* has a *fushi tarazu* homolog expressed in stripes during segmentation. Proc. Natl. Acad. Sci. USA *91*, 12922–12926.

Casso, D., Ramirez-Weber, F., and Kornberg, T.B. (2000). GFP-tagged balancer chromosomes for *Drosophila melanogaster*. Mech. Dev. *91*, 451–454.

Chen, P., Nordstrom, W., Gish, B., and Abrams, J.M. (1996). *grim*, a novel cell death gene in *Drosophila*. Genes Dev. *10*, 1773–1782.

Christich, A., Kauppila, S., Chen, P., Sogame, N., Ho, S.-I., and Abrams, J.M. ((2002). The damage-responsive *Drosophila* gene *sickle* encodes a novel IAP binding protein similar to but distinct from reaper, grim, and hid. Curr. Biol. *12*, 137–140.

Dawes, R., Dawson, I., Falciani, F., Tear, G., and Akam, M. (1994). *Dax*, a locust *Hox* gene related to *fushi-tarazu* but showing no pair-rule expression. Development *120*, 1561–1572.

Delorenzi, M., and Bienz, M. (1990). Expression of Abdominal-B homeoproteins in *Drosophila* embryos. Development *108*, 323–329.

Du, C., Fang, M., Li, Y., Li, L., and Wang, X. (2000). Smac, a mitochondrial protein that promotes cytochrome c-dependent caspase activation by eliminating IAP inhibition. Cell *102*, 33–42.

Garcia-Bellido, A. (1977). Homeotic and atavic mutations in insects. Am. Zool. *17*, 613–629.

Gavalas, A., Davenne, M., Lumsden, A., Chambon, P., and Rijli, F.M. (1997). Role of Hoxa-2 in axon pathfinding and rostral hindbrain patterning. Development *124*, 3693–3702.

Gould, A.P., and White, R.A. (1992). *Connectin*, a target of homeotic gene control in *Drosophila*. Development *116*, 1163–1174.

Goyal, L., McCall, K., Agapite, J., Hartwieg, E., and Steller, H. (2000). Induction of apoptosis by *Drosophila reaper*, *hid* and *grim* through inhibition of IAP function. EMBO J. *19*, 589–597.

Graba, Y., Aragnol, D., and Pradel, J. (1997). *Drosophila* Hox complex downstream targets and the function of homeotic genes. Bioessays *19*, 379–388.

Grether, M.E., Abrams, J.M., Agapite, J., White, K., and Steller, H. (1995). The *head involution defective* gene of *Drosophila melanogaster* functions in programmed cell death. Genes Dev. *9*, 1694–1708.

Handel, K., Grunfelder, C.G., Roth, S., and Sander, K. (2000). *Tribolium* embryogenesis: a SEM study of cell shapes and movements from blastoderm to serosal closure. Dev. Genes Evol. *210*, 167–179.

Hay, B.A., Wassarman, D.A., and Rubin, G.M. (1995). *Drosophila* homologs of baculovirus inhibitor of apoptosis proteins function to block cell death. Cell *83*, 1253–1262.

Hay, B.A., Maile, R., and Rubin, G.M. (1997). P element insertion-dependent gene activation in the *Drosophila* eye. Proc. Natl. Acad. Sci. USA *94*, 5195–5200.

Heuer, J.G., Li, K., and Kaufman, T.C. (1995). The *Drosophila* homeotic target gene *centrosomin* (*cnn*) encodes a novel centrosomal protein with leucine zippers and maps to a genomic region required for midgut morphogenesis. Development *121*, 3861–3876.

Hinz, U., Wolk, A., and Renkawitz-Pohl, R. (1992). Ultrabithorax is a regulator of β3-*tubulin* expression in the *Drosophila* visceral mesoderm. Development *116*, 543–554.

Hu, N., and Castelli-Gair, J. (1999). Study of the posterior spiracles of *Drosophila* as a model to understand the genetic and cellular mechanisms controlling morphogenesis. Dev. Biol. *214*, 197–210.

Hughes, C.L., and Kaufman, T.C. (2002). Exploring the myriapod body plan: expression patterns of the ten *Hox* genes in a centipede. Development *129*, 1225–1238.

Hurle, J.M., Ros, M.A., Climent, V., and Garcia-Martinez, V. (1996). Morphology and significance of programmed cell death in the developing limb bud of the vertebrate embryo. Microsc. Res. Tech. *34*, 236–246.

Jiang, C., Lamblin, A.F., Steller, H., and Thummel, C.S. (2000). A steroid-triggered transcriptional hierarchy controls salivary gland cell death during *Drosophila* metamorphosis. Mol. Cell *5*, 445–455.

Kimmel, B.E., Heberlein, U., and Rubin, G.M. (1990). The homeo domain protein rough is expressed in a subset of cells in the developing *Drosophila* eye where it can specify photoreceptor cell subtype. Genes Dev. *4*, 712–727.

Kurada, P., and White, K. (1998). Ras promotes cell survival in *Drosophila* by downregulating *hid* expression. Cell *95*, 319–329.

Li, K., and Kaufman, T.C. (1996). The homeotic target gene *centrosomin* encodes an essential centrosomal component. Cell *85*, 585–596.

Li, X., Murre, C., and McGinnis, W. (1999). Activity regulation of a Hox protein and a role for the homeodomain in inhibiting transcriptional activation. EMBO J. *18*, 198–211.

Lohr, U., Yussa, M., and Pick, L. (2001). *Drosophila fushi tarazu*: a gene on the border of homeotic function. Curr. Biol. *11*, 1403–1412.

Mann, R.S., and Affolter, M. (1998). Hox proteins meet more partners. Curr. Opin. Genet. Dev. *8*, 423–429.

Mann, R.S., and Morata, G. (2000). The developmental and molecular biology of genes that subdivide the body of *Drosophila*. Annu. Rev. Cell Dev. Biol. *16*, 243–271.

McGinnis, W., Jack, T., Chadwick, R., Regulski, M., Bergson, C., McGinnis, N., and Kuziora, M.A. (1990). Establishment and maintenance of position-specific expression of the *Drosophila* homeotic selector gene *Deformed*. Adv. Genet. *27*, 363–402.

Meadows, L.A., Gell, D., Broadie, K., Gould, A.P., and White, R.A. (1994). The cell adhesion molecule, *connectin*, and the development of the *Drosophila* neuromuscular system. J. Cell Sci. *107*, 321–328.

Meier, P., Silke, J., Leevers, S.J., and Evan, G.I. (2000). The *Drosophila* caspase DRONC is regulated by DIAP1. EMBO J. *19*, 598–611.

Nassif, C., Daniel, A., Lengyel, J.A., and Hartenstein, V. (1998). The role of morphogenetic cell death during *Drosophila* embryonic head development. Dev. Biol. *197*, 170–186.

Patel, N. (1994). The evolution of arthropod segmentation: insights from comparisons of gene expression patterns. Dev. *Suppl*., 201–207.

Peterson, C., Carney, G.E., Taylor, B.J., and White, K. (2002). *reaper* is required for neuroblast apoptosis during *Drosophila* development. Development *129*, 1467–1476.

Pradel, J., and White, R.A. (1998). From selectors to realizators. Int. J. Dev. Biol. *42*, 417–421.

Raghavan, S., and White, R.A. (1997). *Connectin* mediates adhesion in *Drosophila*. Neuron *18*, 873–880.

Rubin, G.M., and Spradling, A.C. (1982). Genetic transformation of *Drosophila* with transposable element vectors. Science *218*, 348–353.

Sanchez-Herrero, E., Vernos, I., Marco, R., and Morata, G. (1985). Genetic organization of *Drosophila bithorax* complex. Nature *313*, 108–113.

Sanson, B., White, P., and Vincent, J.P. (1996). Uncoupling cadherin-based adhesion from wingless signalling in *Drosophila*. Nature *383*, 627–630.

Saunders, J.W., and Fallon, J.F. (1966). Cell death in morphogenesis. In Major Problems in Developmental Biology, M. Locke, ed. (New York: Academic Press), pp. 289–314.

Schmidt-Ott, U., and Technau, G.M. (1992). Expression of *en* and *wg* in the embryonic head and brain of *Drosophila* indicates a refolded band of seven segment remnants. Development *116*, 111–125.

Srinivasula, S.M., Datta, P., Kobayashi, M., Wu, J.-W., Fujioka, M., Hegde, R., Zhang, Z., Mukattash, R., Fernandes-Alnemri, T., Shi, Y., et al. (2002). *Sickle*, a novel *Drosophila* death gene in the *reaper/hid/grim* region, encodes an IAP-inhibitory protein. Curr. Biol. *12*, 125–130.

Stadler, H.S., Higgins, K.M., and Capecchi, M.R. (2001). Loss of Eph-receptor expression correlates with loss of cell adhesion and chondrogenic capacity in *Hoxa13* mutant limbs. Development *128*, 4177–4188.

Suzuki, Y., Imai, Y., Nakayama, H., Takahashi, K., Takio, K., and Takahashi, R. (2001). A serine protease, HtrA2, is released from the mitochondria and interacts with XIAP, inducing cell death. Mol. Cell *8*, 613–621.

Telford, M.J. (2000). Evidence for the derivation of the *Drosophila fushi tarazu* gene from a *Hox* gene orthologous to lophotrochozoan *Lox5*. Curr. Biol. *10*, 349–352.

Vachon, G., Cohen, B., Pfeifle, C., McGuffin, M.E., Botas, J., and Cohen, S.M. (1992). Homeotic genes of the *Bithorax* complex repress limb development in the abdomen of the *Drosophila* embryo through the target gene *Distal-less*. Cell *71*, 437–450.

Verhagen, A.M., Ekert, P.G., Pakusch, M., Silke, J., Connolly, L.M., Reid, G.E., Moritz, R.L., Simpson, R.J., and Vaux, D.L. (2000). Identification of DIABLO, a mammalian protein that promotes apoptosis by binding to and antagonizing IAP proteins. Cell *102*, 43–53.

Wang, S.L., Hawkins, C.J., Yoo, S.J., Muller, H.A., and Hay, B.A. (1999). The *Drosophila* caspase inhibitor DIAP1 is essential for cell survival and is negatively regulated by HID. Cell *98*, 453–463.

White, K., and Steller, H. (1995). The control of apoptosis in *Drosophila*. Trends Cell Biol. *5*, 74–78.

White, K., Grether, M.E., Abrams, J.M., Young, L., Farrell, K., and Steller, H. (1994). Genetic control of programmed cell death in *Drosophila*. Science *264*, 677–683.

Wing, J.P., Karres, J.S., Ogdahl, J.L., Zhou, L., Schwartz, L.M., and Nambu, J.R. (2002). *Drosophila sickle* is a novel *grim-reaper* cell death activator. Curr. Biol. *12*, 131–135.

Yoffe, K.B., Manoukian, A.S., Wilder, E.L., Brand, A.H., and Perrimon, N. (1995). Evidence for engrailed-independent *wingless* autoregulation in *Drosophila*. Dev. Biol. *170*, 636–650.